[Reprinted from CLINICAL CHEMISTRY, 28, 840 (1982).]

Some Extensions to the GELLAB Two-Dimensional Electrophoretic Gel Analysis System

P. F. Lemkin,[1] L. E. Lipkin,[1] and E. P. Lester[2]

Several important extensions to the GELLAB 2D electrophoresis gel analysis system are discussed, including concepts that lead to the generation of consistent gel maps for a particular cell line, as illustrated by some recent results for the P388D1 cell system. GELLAB is an interactive graphics computer system that facilitates (*a*) image accessioning, (*b*) spot-data extraction from the image with position and density quantitation, (*c*) pairing of corresponding spots between gels, and (*d*) spot analysis for a large number of corresponding spots (over 3000 per gel) for up to 128 gels. Multiple gels are accessioned into the system used to create a composite gel data base. These then may be partitioned into multiple classes of gels and searched for statistically significant interclass spot differences, which can be visualized in reference map images of selected spot sets as well as mosaic images of particular spots in all gels. In addition to the visual feedback that is available during the gel analysis, various statistical, numerical, and other displays may be generated in the CGELP interactive program of the GELLAB system.

Additional Keyphrases: *data processing* · *computer analysis* · *canonical gel maps* · *gel pairing* · *data base management*

Two-dimensional electrophoresis on polyacrylamide gels (2D PAGE) (*1*) has proven to be an extremely powerful investigative tool for the biomedical researcher (*2*).[3] In this paper we discuss several important extensions to the GELLAB system that is used for the analysis of such gels (*3–10*).

But before describing these extensions, we will review some of the details of GELLAB, which is a 2D PAGE image-analysis system, realized as a set of programs that are run on DECsystem-10 or DECsystem-20 computers. Briefly, 2D gels with patterns made visible as autoradiographs or photographs are assigned sequential accession numbers in the system and then converted to digital images by one of several methods, such as with a television camera or an Optronics scanner. These gel images are then analyzed, by use of the SG2DRV program (*3, 6, 9*). This extracts the spots from each gel and denotes each spot by a set of features including *x* (isoelectric point) and *y* (molecular mass) location, area, and integrated density. Morphologically distinctive landmark spots are identified on each gel by using either interactive computer graphics techniques (*4, 6, 9*) or manual observation and data entry from plots of spots for each gel (*cf. Discussion*). By using the gel spot lists and landmarks, all possible spots are paired by the CMPGEL program, between each gel and a *representative gel*, or *R-gel* (*5, 6, 9*). The composites of such paired spot sets (across all gels) are called *representative spot* (or *R-spot*) *sets*. These are then used to construct a *composite gel* (CGL) data base which may be analyzed in many ways. Each R-spot set, as it is formed, is assigned an arbitrary sequential numeric name. At this stage of the analysis, GELLAB, via the CGELP interactive program, permits partitioning by spot features or classes of experimental gels. Extensive statistical, numerical, and display tools for data base treatment are also provided. Up to 3000 R-spot sets for up to 128 gels may be created with the current GELLAB data-base system.

GELLAB is a continuously evolving system for 2D gel analysis. Several extensions, discussed here, have been made to the system as previously described (*3–5*). These extensions, taken together, result in a system that is both easier for the biologist to use and more effective and inclusive for spot analysis and accounting.

At an early stage in spot-integrated density quantitation, some correction of spot-integrated density measurements is necessary, to take "background" density into account. Several algorithms are available for estimating corrected spot-integrated density, ranging from relatively simple subtraction of the local surrounding density to globally based density corrections. Here we present a modification of the zonal notch filter (*12, 13*) and illustrate how it provides a better estimate of background than did our previous technique (*3*).

Heretofore it was possible that for a given CGL data base, a set of congeneric spots (i.e., spots on separate gels that represent the same thing) was not accessible to analysis, if by chance the spot was not present in the gel chosen as the R-gel. Spots that do not pair with a spot in the R-gel are designated as *unresolved spots*, labeled with the US symbol (*4, 8, 9*). The set of extensions we are presenting here correct this deficiency. In this connection we introduce the concept of the *extended R-spot* (*eR-spot*) set.

This enhanced capability of dealing with a more nearly complete set of spots from gel to gel allows us to pursue the idea of a *canonical gel*, "C-gel", (in the sense of a standard catalog) and to approach this theoretical construct more closely than heretofore (*4, 6, 9*). We are now able to introduce the concept of a *C-gel′*, an estimate of the canonical gel based on the averages of R-spot sets of replicate gels. The procedures used in creating the C-gel′ provide for the exclusion of spots that are poorly represented in any replicate set and of most "noise spots" and other artifacts.

Finally, GELLAB provides a greatly expanded and explicit package of set theoretic operations, which may be applied to sets of spots delineated by particular statistical conditions or constraints. We demonstrate the utility of these operations for identifying interesting biological events in multidimensional (i.e., multiple experimental class) data bases.

[1] Image Processing Section, Division of Cancer Biology and Diagnosis, National Cancer Institute, National Institutes of Health, Bethesda, MD 20205.

[2] Department of Medicine, Section of Hematology/Oncology, University of Chicago Medical School, Box 420, 950 East 59th St., Chicago, IL 60637.

Address correspondence to P.F.L. at: Park Bldg., Room 417, N.I.H., Bethesda, MD 20205.

[3] Nonstandard abbreviations: 2D, two-dimensional; PAGE, polyacrylamide gel electrophoresis; CGL, composite gel; US, unresolved spots; R-spot, representative spot; eR-spot, extended R-spot; C-gel, canonical gel; C-gel′, an estimate of the canonical gel based on the R-spot sets of replicate gels; DP, distance between two paired spots mapped to the same domain; EP, extrapolated pair; D′, the mean R-set set-integrated spot density; GSF, gel-segmentation file; GCF, gel-comparison file; LMS′, landmark set; and SRL, Search Results List.

Methods

Extension of CGL Data Base to Include Extended R-spots

Figure 1 illustrates the case in which certain spots are present in a set of gels, but not in the R-gel. As mentioned, spots that do not pair with those in the R-gel are called "unresolved spots" (US). The extended R-spot set construction handles this missing spot problem by creating eR-spot sets based on the US spots.

The initial R-spot data base is first constructed to contain all R-spots as described in references *5* and *9*. It does not contain these missing US spots at this initial stage. The set of paired spot files is then scanned a second time for those US spots *not* in the R-gel that are "robust"—i.e., that have reasonable values for selected spot features (total area, integrated density, and density range—i.e., max-min optical density or absorbance) within the limits set by the experimenter. When a non R-gel US spot is read from a paired spot list file, it is first tested to see whether it belongs to an existing eR-spot set. Its coordinates are then mapped to the domain of the R-gel where the nearest existing eR-spot coordinates are found. The mapping function is simply the linear landmark transformation for mapping a landmark spot in the gel to the same landmark in the R-gel. The particular landmark transformation used for a given US spot is that of the (nearest) landmark set to which the US spot belongs.

For example, given a spot's centroid (density weighted center) and landmark (x,y) coordinates for its (nearest) landmark set k in both the R-gel and in gel g, the linear transformation to the domain of the R-gel for this gel-g spot is defined as follows. Let $(x,y)_{\mathrm{LM}[g,k]}$ be the landmark coordinates of gel g landmark k. Then the mapped centroid is defined in vector notation,

$$(x,y)'_{\text{R-gel}} = (x,y)_{g} + (x,y)_{\mathrm{LM}[\text{R-gel},k]} - (x,y)_{\mathrm{LM}[g,k]}$$

The $(x,y)'$ is then tested to determine whether the spot lies within DP limits of the nearest eR-spot in the R-gel, DP being defined as the distance between two paired spots mapped to the same domain (i.e., R-gel), (*cf. 4, 8, 9*). If the US spot meets this test, it is then put into that eR-spot set. If not, a new eR-spot set is created along with an *extrapolated pair* (EP) spot label with zero density for the R-gel itself. Note that the number names denoting eR-spots are treated the same as those of normal R-spots for all purposes in analyzing a CGL data base. However, eR-spots have only EP and US spot-pairing labels.

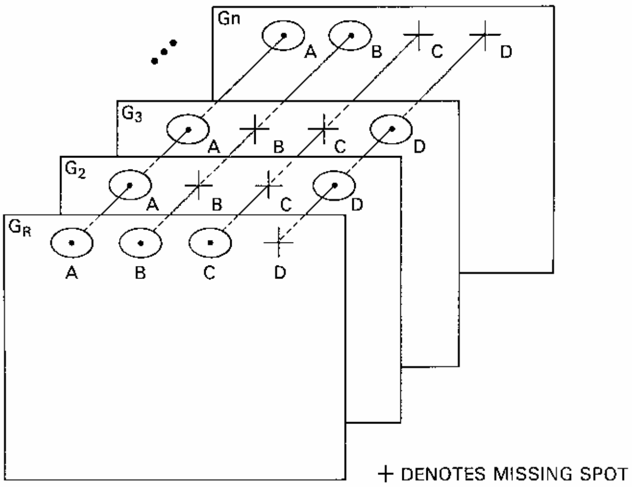

Fig. 1. Example of the occurrence of the pairing of spots between gels (Gr, G2 to Gn)

Spot *A* occurs in *all* gels; spot *B* in the R-gel and *some* of the other gels; spot *C only* in the R-gel (i.e., US spot in the R-gel); Spot *D* in some of the other gels but *not* in the R-gel (i.e., US spots in other gels). Spots *A, B, and C* would be found as un-extended R-spots; spot *D* would be an eR-spot

Extension of CGL Data Base to Generate and Use the C-gel′

One can compute an estimate of a C-gel (*5–9*) from the CGL data base under particular conditions. This estimate, called the C-gel′, is usually derived from a set of replicate gels. By "replicate" we mean 2D gel patterns produced from the same sample or from parallel tissue cultures, run concurrently under the same conditions. Having created such a CGL data base, feature sizing as described earlier (*5, 9*) is used to discriminate spots from noise. R-spot sets that meet this sizing test are called "C-spot′ sets." For example, requiring that 80% of the gels contain the given R-spots and that the coefficient of variation (CV) of R-spot set density be less than some small value would find robust C-spot′ estimates in most of the gels. The C-gel′ is defined to have the same accession number as the R-gel in this replicate gel, set, *but* the accession number (*3*) extension (i.e., decimal fraction part) is defined to be "9" (e.g., R-gel accession number 250.2 would have the derived C-gel′ accession number 250.9). (Otherwise, the accession number extension is usually used to distinguish among different radioautographic exposures for a *given* gel.)

A composite (synthetic) GSF′ file for a set of replicate gels is then produced, in which the mean R-spot set centroid (x,y) mapped *onto* the R-gel is used as well as the mean R-spot set-integrated spot density D′ [background-corrected original density measurement in optical density units (*3*)] and the area. The standard deviations of these variables and the number of gels per R-spot set are also entered into this file for later use in building (and for performing statistical tests with) a new CGL′ data base that is based on the C-gel′. Spots are renumbered sequentially from 1 where only those spots meeting the feature-sizing criteria are included. This procedure uniquely defines a set of C-gel′ spots. Figure 2 illustrates the mapping of replicate gels onto the R-gel during creation of the C-gel′.

During C-gel′ generation, the landmark data base (*4, 9*) is searched for matching (R-gel, gel g) entries for all gels g—i.e., matched against the same given R-gel. (The landmark data base consists of a list of landmark sets for various R-gel/gel-g pairs. A particular landmark set of paired spots for each gel g paired with R-gel typically contains 10 to 25 pairs of specific spot (x,y) coordinates for the two gels). A modified duplicate

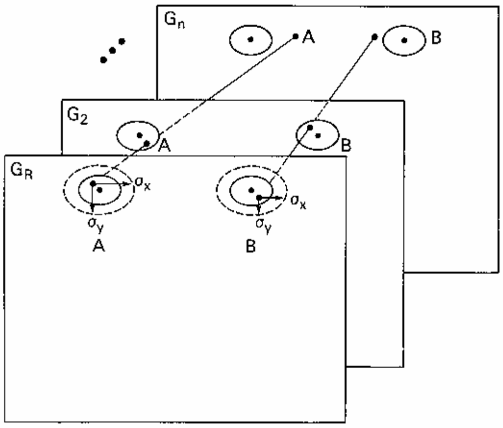

Fig. 2. Example of mean spots computed by projecting spots from replicate gels *onto* the domain of the R-gel

When that has been done, means and standard deviations of *x* centroid, *y* centroid, density, and area may be computed. Such mean spots estimated from replicate gels are called synthetic C-gel′ spots (i.e., *estimates* of the canonical gel) of each matched landmark set is inserted into the landmark data base file, where the R-gel name is changed to that of the C-gel′ and the mean centroids of the C-spot′ landmark spots are substituted for the corresponding R-gel landmark spots. The C-gel′ analysis typically proceeds as follows.

Constructing the Initial C-gel′

(1) Accession a data base consisting of replicate control gels.
(2) Landmark all gels to one of the replicate gels (i.e., define one as the R-gel). Segment all gels to get the spot feature lists in the *gel-segmentation files* (GSF) (*3, 6, 9*).
(3) Build a CGL data base (*5, 6, 9*) from these replicate gels by pairing these gels to produce *gel-comparison files*, or GCF (*6, 9*). These GCF files are then used to build the CGL data-base consisting of R-spot and eR-spot sets.
(4) Pick R-spot set feature sizing parameters in order to recognize robust R-spot sets to be defined as C-spot′ sets.
(5) Create the C-gel′ synthetic GSF′ and LMS′ data base files as detailed above.

Analyzing New Experimental Gels in the Context of the C-gel′

(1) Accession new experimental gels.
(2) Landmark these to C-gel′ (visualized in and using the R-gel for landmarking purposes).
(3) Segment (i.e., extract spot features for) these gels into a set of GSF files. Then, pair spots on these gels with the previously generated C-gel′ GSF′ file, resulting in a set of GCF′ files.
(4) Build and analyze a CGL′ data base by using these new GCF′ files.

Once the CGL′ data base is constructed, it has the following characteristics, illustrated in Figure 3: (*a*) all C-gel′ spots are normal R-spot sets (i.e., not eR-spots); (*b*) all experimental gel US spots are in eR-spot sets (i.e., spots missing in C-gel′); (*c*) all paired (paired with C-gel′ synthetic spots) experimental spots are in the normal R-spots sets; (*d*) any C-gel′ spots *not* in the experimental gels are normal R-spot sets consisting of one US spot (i.e., spots missing in the experimental gel); (*e*) the C-gel′ may be used later with *additional* replicate gels to build a *new* C-gel′ estimate. This iterative process gradually may lead to better and better estimates of the canonical gel; and (*f*) if *all* gels of a particular domain are merged together, then a C-gel′ results that represents those spots found in all of the gels, or at least in a given percentage of them (as defined by the user).

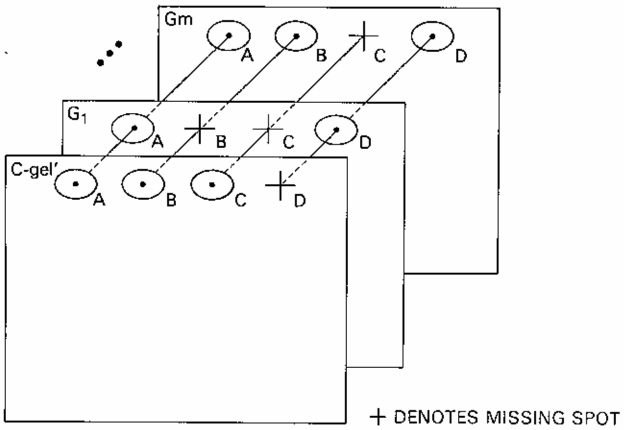

Fig. 3. Example of the occurrence of spots between the synthetic C-gel′ and a set of experimental gels (G1 to Gn)

Spots *A, B, and C* are R-spots found in C-gel′; spot *D* is an eR-spot *not* found in C-gel′. Therefore, spot *C* would be a spot found *only* in the experimental gels

When the C-gel′ data are read back into the CGL′ data base during the creation of the experimental data base, the standard deviations of C-spot′ (*x* centroid, *y* centroid, density, area) and the number of gels per C-spot′ set estimate are saved for each C-spot′. Their mean values now become the C-spot′ estimates for these features. These features have been passed from the synthetic GSF′ file through the synthetic GCF′ files now being used to create the CGL′ data base. These data (means, standard deviations, and number of gels per C-spot′ set) are of course available for use in any statistical test with the experimental gels that later is performed in CGELP.

To summarize, a single partition exists whereby missing spots in either gel may easily be identified as being US spots in R-spot or eR-spot sets corresponding to spots missing in the experimental or C-gel′ gels, respectively. By definition, all eR-spot set numbers are those higher than the last normal R-spot set number—either of which may be analyzed by the user at any time in a given CGL data base.

A special case occurs when a data base is built by use of the C-gel′ and the original replicate gels. To see how well one did in constructing the C-gel′, one can build a CGL′ data base with it and with the original replicate gels. Any eR-spot sets that occur are US spots where the original R-spot or eR-spot sets were sized out during the creation of C-gel′. There can be no US spots in the un-extended R-spot sets.

Use of Sets in GELLAB

GELLAB permits manipulation of sets of *gel names*, first mentioned in ref. *5*. These may be defined and manipulated with the usual set theoretic operations of union, intersection, and non-commutative set substraction (*11*). This is useful when one is investigating many gels consisting of several observational classes or in redefining the *working set of gels* by subset name(s). The working set of gels is defined to be a subset of the set of all gels in the current CGL data base.

Similarly, lists of selected R-spots may be manipulated. Such a list is called the *Search Results List* (SRL) and is generally the result of applying some statistically driven search over the R-spot CGL data base (*5, 8, 9*). The tools available on which search strategies may be based include multi-class *t*-, *F*-, and rank-order tests as well as R-spot set feature sizing against user-specified limits. The particular subset of gels considered for a given search may be altered by the user specifying the current "working set of gels" before the search. Because each element of the SRL appears only once, it may be treated as a set, e.g.,

{R-spot$_i$, R-spot$_j$, . . . R-spot$_p$}.

An example of an R-spot set (*cf.* Figure 5) is:

{48, 58, 60, 162, 220, 223, 230, 231, 233, 592}.

SRL subsets may thus be defined as the current SRL (possibly the result of the last search), explicitly by the user or as the result of one of the usual set theoretic operations (union, intersection, non-commutative subtraction). Any SRL subset may be used to redefine the current (i.e., the "working") SRL.

The set of R-spots so defined may be used for all of the operations available for the SRL (*5, 8, 9*). These include: (*a*) creation of data files for statistical analysis with a non-GELLAB statistical package such as SPSS (*21*), generation of R-map images or plots where spots of interest are labeled on the image, and (or) generation of mosaic images or plots consisting of panels surrounding a particular R-spot for all gels in the data base; (*b*) computing the ratio histogram of selected spots (the ratio is of the mean densities of two classes); (*c*) printing the rank-order table (plotting spot densities for each of the gels as a function of R-spot); and (*d*) normalizing or re-normalizing the CGL data base by use of the total D′ of R-spots in the SRL for each gel.

Use of Search Results List Set Operations in Analyzing the Data Base

Two experimental designs are given here to illustrate the application of set theory considerations to SRL subsets.

Example 1. In analyzing a multi-dimensional gel data base (i.e., several different classes of observations of experimental gels), spots found in one pairwise classification might be compared with spots found in another. For example, (Control vs Treatment 1) vs (Control vs Treatment 2). Spot differences found in the gels after both treatments are the intersection of the two searches. Spots found only in Treatment 1 are the set difference computed by removing Treatment 2 spots that are also present after Treatment 1. Spots found after either treatment are the set union.

Example 2. In a time-sequence or drug-concentration experiment, one might ask questions about which spots first appear or increase, increase some more, and then decrease or even disappear—signaling gene expression under a particular set of conditions. The CV for R-spot set density would be large at the transition zones—and possibly large in between, depending on the shape of the curve for spot density. The case where the CV is stable in the growth curve can easily be detected with GELLAB by searching for spots for which the CVs are small. Changing spots can be found by searching with a high CV value constraint (R-spot sets with a large CV but a small mean D′ can be ignored to help decrease the false-positive rate). Taking this last case, one could find the sequence of gels with such variable spots as follows.

(1) Given k gels (or gel experimental classes, possibly with multiple samples in each class) in the sequence, find the intersection of SRL subsets for each two sequential classes, with the constraint that a spot is considered if its CV exceeds some specified value. The resulting SRLs are saved as k − 1 SRL subsets

$$\{S_1, S_2, \ldots S_{k-1}\}.$$

That is,

$$S_i = \mathrm{SRL}_i \text{ UNION } \mathrm{SRL}_{i+1}$$

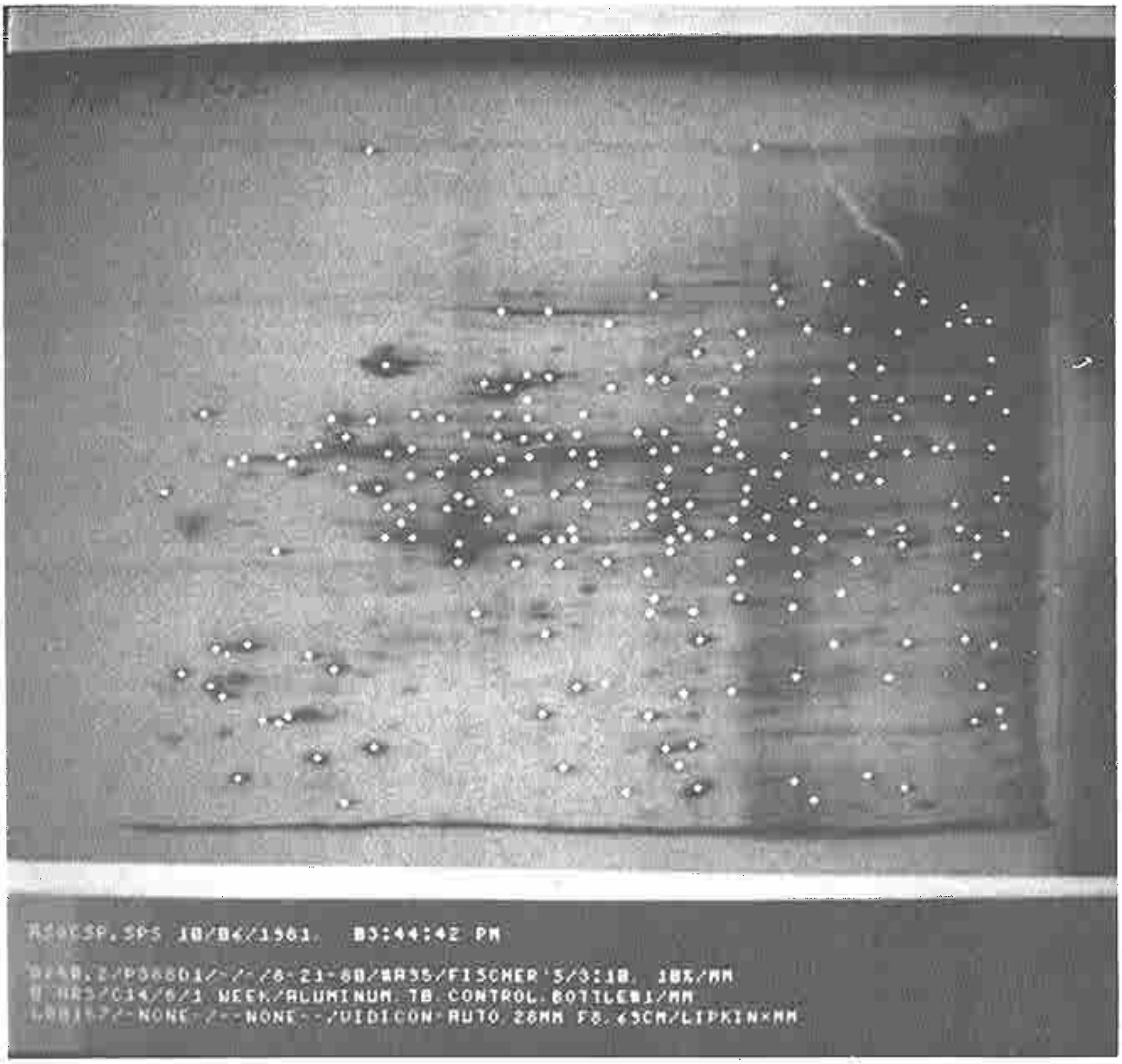
RSOCSP.SPS 10/04/1981 03:44:42 PM
0?AR.2/P388D1/-/-/6-21-80/WA35/FISCHER 5/3:10 10%/MM
MR5/C14/6/1 WEEK/ALUMINUM TB CONTROL BOTTLE#1/MM
-NONE-/--NONE--/VIDICON AUTO 28MM F8 45CM/LIPKIN×MM

Fig. 4. R-map image of C-gel′ for eight replicate gels of a P388D1 mouse macrophage-like cell line

The replicates were from eight tissue-culture bottles. The spots included in the C-gel′ are marked (in white, here) with "+" and were those present in at least six of the eight gels

Table 1. Two-class Ratio Histogram Table of Selected R-Spot Sets from the *t*-Test Search at .95 Significance [a]

Found 10 R-spots, mean SD/mn (for entire R-spot set) = .35 ± .11

m2/m1	R-spot sets
1.40	162 231
1.45	233
1.50	
1.55	
1.60	48 592
1.65	223 230
1.70	
1.75	58 220
1.80	
1.85	
1.90	
1.95	
2.00	
2.05	
2.10	
2.15	
2.20	60

[a] The ratio m2/m1 is computed from the mean density values of the two classes T_0 and T_{24} (class 1 and 2, respectively) for each R-spot set selected.

(2) For each S_i, compute the *sequential intersection* SI_{iw} as follows:

$$SI_{iw} = \text{UNION } S_j \quad j = i \text{ to } i + (w - 1).$$

Thus SI_{iw} is the intersection of a sequence of subsets starting at SRL subset i and looking forward through w subsets. This sequential intersection may be computed manually in GELLAB by using a composition of the UNION SRL subset operation on two sets at a time. It may also be more easily specified using the SEQUENTIAL INTERSECTION operator, which takes two arguments: starting SRL subset number i and number of subsets width w. A further extension of the sequential intersection operator computes all of the SI_{iw} for g SRL subsets and for i ranging from 1 to (g − 1) − (w − 1)). By applying this last operation for several sizes of w (i.e., w = 2, 3, . . . , g − 1), any occurrence of spots appearing in any S_i through S_{i+w-1} for any interval w is detected.

Use of the Zonal Notch Filter for Estimating Gel Background Density

In previous papers (*3*, *14–18*, *22*), various methods have been used for estimating gel image background density. Knowing this local background density value enables one to correct the measured integrated density D to an integrated density D′ by using the transformation [valid for small maximum picture element (pixel) optical-density values]:

$$D' = D - (\text{mean background density per pixel} \times \text{total spot area, in pixels}).$$

In the new method described here, information about extracted spots is taken into account when background density is estimated. The technique involves use of the zonal notch filter (*12*, *13*) by considering pixel-density values that lie within a particular pixel density range (i.e., "zone") to be the background region. The method, as modified here, re-defines this density zone as that part of the gel image where there are no spots. This definition has the advantage over the classic zonal threshold algorithm of being dependent on subject domain (i.e., spot) context. Both major streaks and slowly varying subtle background shading are considered to be background. At each pixel in the image, an average of N × N neighborhood pixel density is computed for those pixels in the square that are not part of extracted spots. Processing proceeds line by line, left to right, adding the next right-most column sum and subtracting the left-most minus one column sum (keeping track of the number of non-spot pixels per window). Thus the N × N pixel average need not be computed explicitly at each pixel. Whether a pixel is a background or resolved-spot pixel is assessed by testing against the propagated central core image (*3*, *6*, *9*) previously generated during gel spot segmentation. The zonal notch filter value at the centroid position of a spot is used as the estimate of its background density. An example of the application of the zonal notch filter is shown in the *Results*.

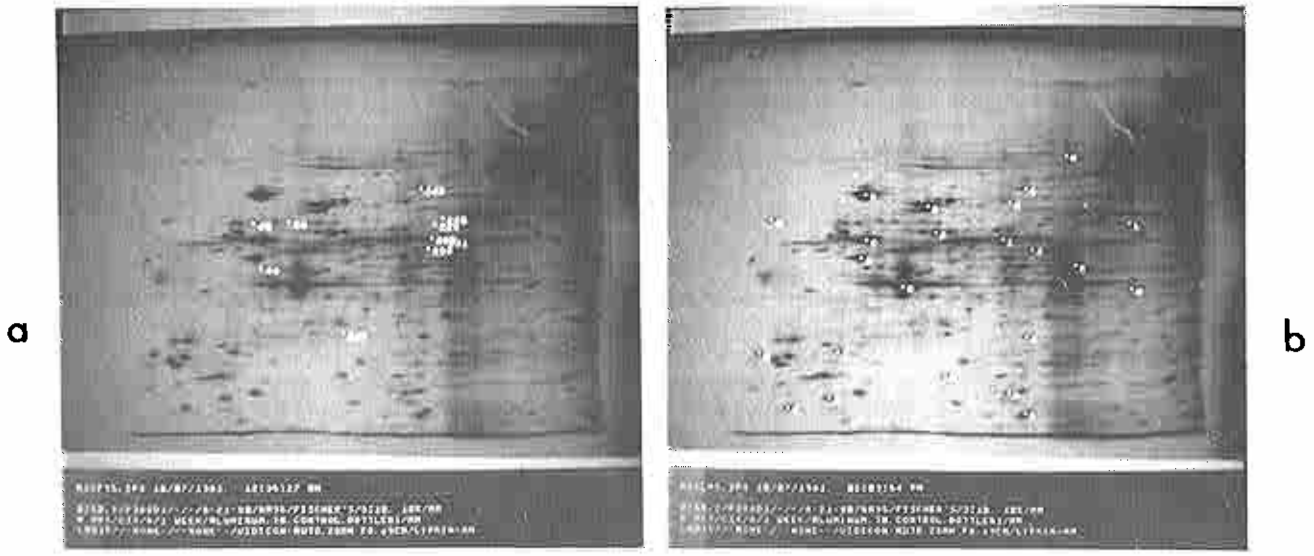

Fig. 5. R-maps of (*a*) set of landmark spots used in pairing of the data base and (*b*) selected R-spots in a set of P388D1 macrophage-like cells that showed .95 significance in mean density difference in particular spots over time as defined by the *t*-test
The two classes are T_0 and T_{24} (24 h later)

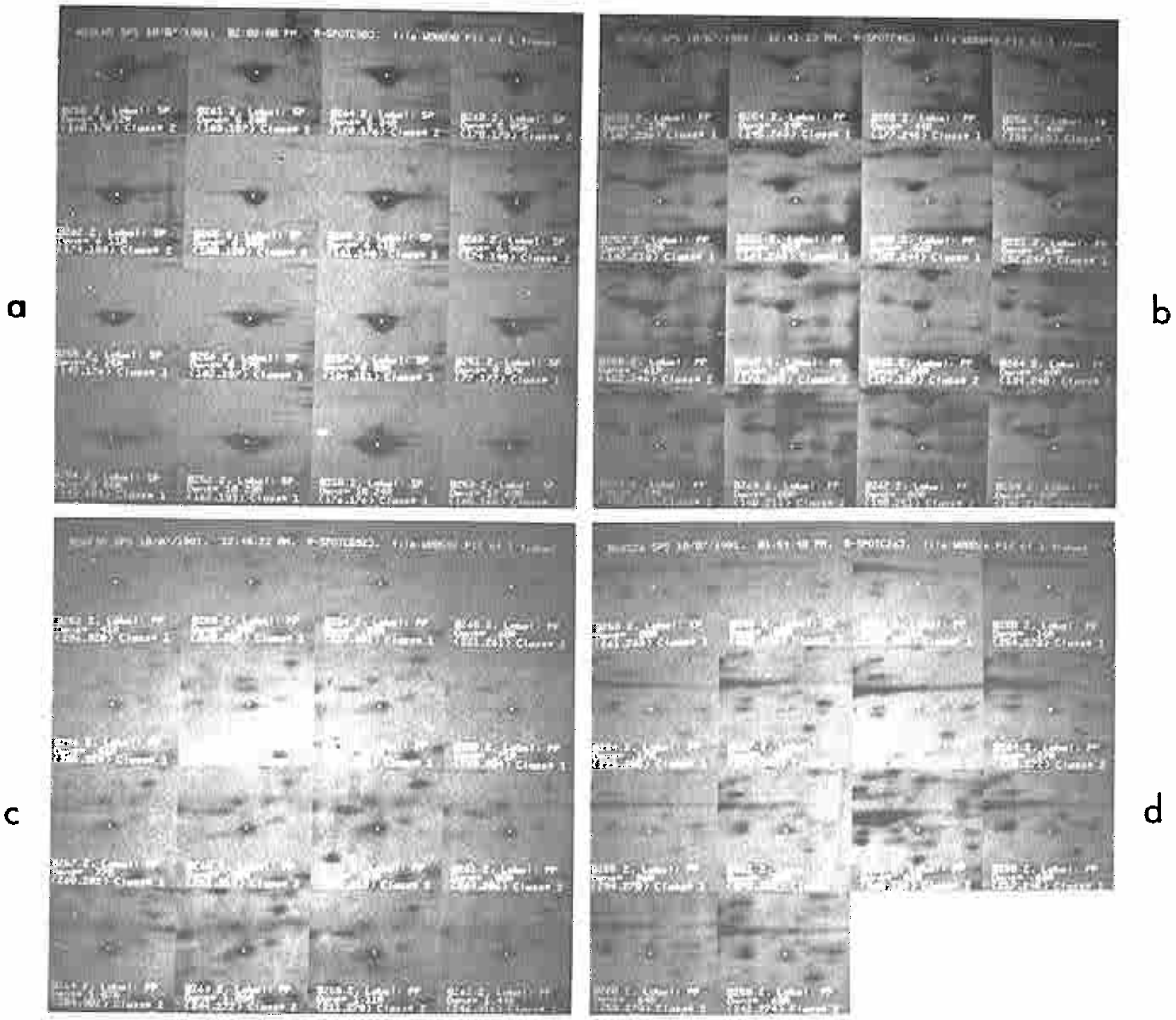

Fig. 6. Examples of mosaics of some of the spots found in the P388D1 CGL data base time-difference study

Class 1 is T_0 and class 2 is T_{24}. Pairing labels are *SP*, sure pair; *PP*, possible pair; *EP*, extrapolated pair. (*a*) Mean density $T_0 >$ mean density T_{24} for R-spot 90, which is landmark *D*; (*b*) and (*c*) mean density $T_{24} >$ mean density T_0 for R-spots 48 and 592, respectively; and (*d*) example of extrapolated pair (EP) spots where spot is not there or is very light—R-spot 26

Results

The following results are those we found for differences over time in the P388D1 mouse macrophage-like cell line (*8*, *23*). This cell line is extensively used in our laboratory to study the cytotoxicity of durable fibers such as asbestos, aluminum oxide, and other fibers. The cells were grown in tissue culture in L-leucine-deficient Fischer's medium (GIBCO no. 80-0039) with 50 μCi of ^{14}C-labeled L-leucine added per culture bottle. Initially half of the 16-culture set was harvested at time T_0 and the other half 24 h later (time T_{24}). The 100 g/L polyacrylamide gels were run in an Ampholine pH range of 3–10 according to the O'Farrell technique (*1*), by David Goldman and Carl Merril of NIMH. One-week exposures of the autoradiographs were used.

Figure 4 shows a C-gel′ R-map image of the eight T_0 replicate gels with all spots marked that were included in the C-gel′. The sizing constraints were that an R-spot had to be in six of the eight replicate gels in order to be considered a C-spot′.

We computed a two-class ratio histogram showing mean densities for the R-spot sets found by the *t*-test search of the P388D1 CGL data base at 95% significance. For each R-spot set resulting from the search, the mean density m2 for spots in class 2 (T_{24}) gels is divided by the mean density m1 of spots class 1 (T_0) gels. The R-spot set name (R-spot number) is entered in the histogram table. Table 1 shows the histogram data for the above *t*-test.

Figure 5*a* illustrates some of the R-spot sets found to differ statistically significantly with time during one of the *t*-test searches. Figure 5*b* illustrates the set of landmark spots, labeled with letter names, used in spot-pairing between the gels. Figure 6 illustrates mosaic images of some of the spots found in the *t*-test. Figure 6*a* shows a spot (landmark D) where the polypeptide decreased with time. Figure 6*b* through 6*d* illustrate polypeptides that increased with time. In Figure 6*d* the spot was in fact missing in two of the gels; the spots were extrapolated in these gels (in the upper leftmost two panels) by use of the CGELP program. Such extrapolated spots can be used to aid in verifying that the missing spots were either not there, were very light (i.e., below detectability with the visualization system), or were mis-paired.

Figure 7*a* illustrates an original P388D1 T_0 gel image, 7*b* its segmented (i.e., extracted spots) image, and 7*c* the background image constructed by subtracting the segmented

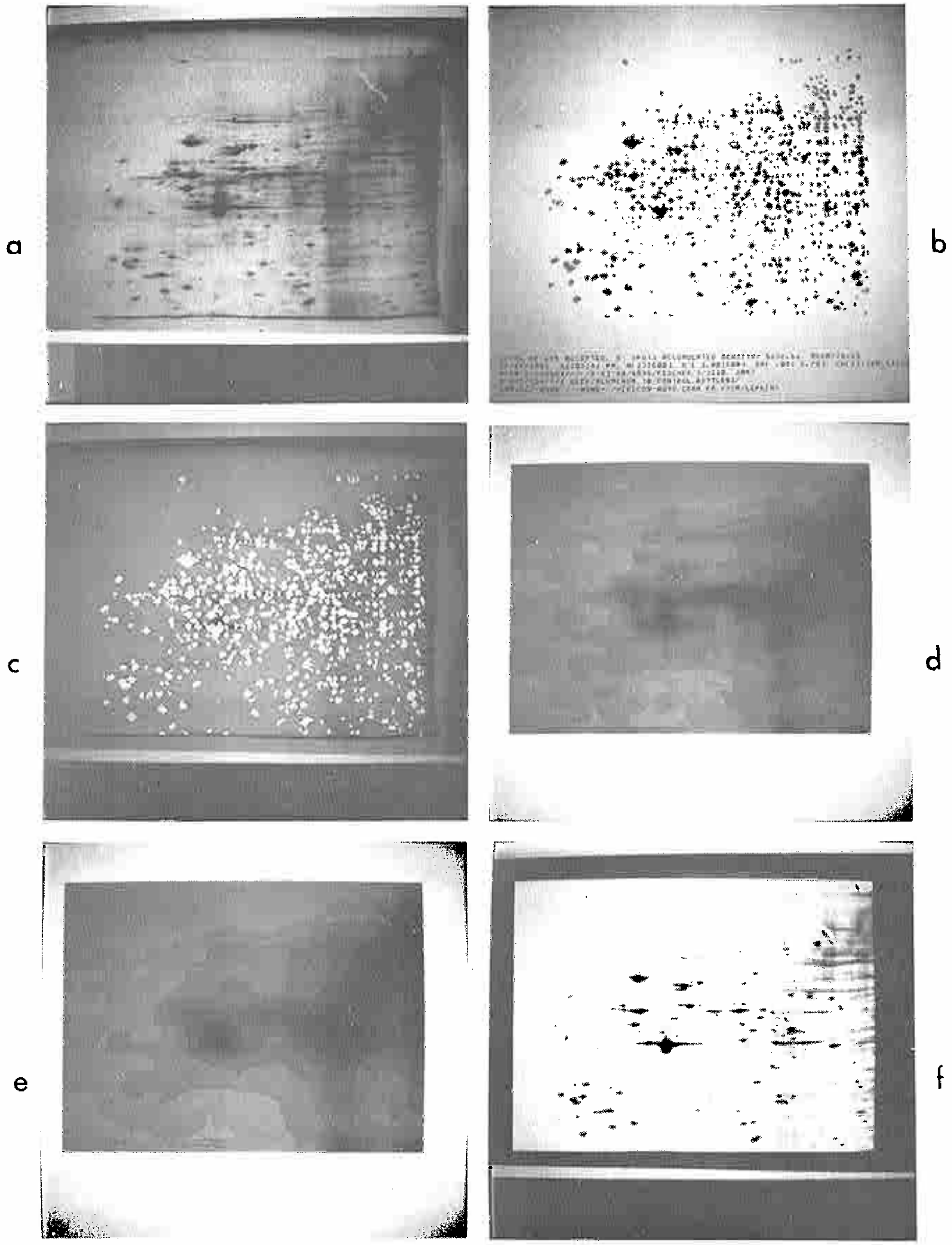

Fig. 7. Example of the modified zonal notch filter used to estimate gel image background density

(*a*) original image of a P388D1 T_0 gel; (*b*) segmented spot image of *a*, showing spots extracted; (*c*) difference image computed by subtracting *b* from *a*; (*d*) zonal notch filter of size 16 × 16 pixels computed for *c*, where zero (white) pixels are ignored in computing the average; (*e*) zonal notch filter of size 32 × 32; and (*f*) original image *a*, less 32 × 32 zonal notch filter *e*

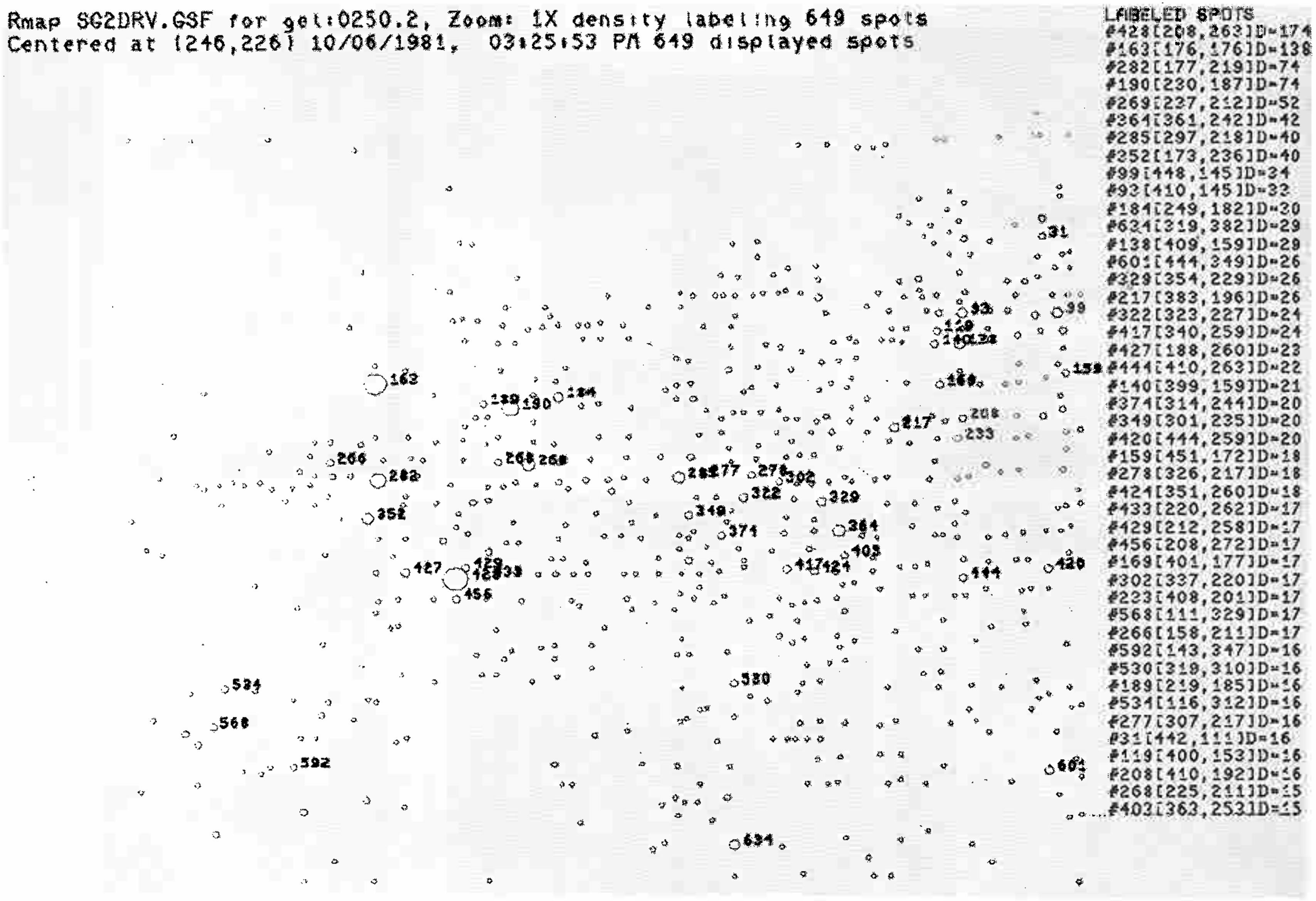

```
Rmap SG2DRV.GSF for gel:0250.2, Zoom: 1X density labeling 649 spots
Centered at [246,226] 10/06/1981,  03:25:53 PM 649 displayed spots
```

```
LABELED SPOTS
#428[208,263]D=174
#163[176,176]D=138
#282[177,219]D=74
#190[230,187]D=74
#269[237,212]D=52
#364[361,242]D=42
#285[297,218]D=40
#252[173,236]D=40
#99[448,145]D=34
#93[410,145]D=32
#184[249,182]D=30
#624[319,382]D=29
#138[409,159]D=29
#601[444,349]D=26
#329[354,229]D=26
#217[383,196]D=26
#322[323,227]D=24
#417[340,259]D=24
#427[188,260]D=23
#444[410,263]D=22
#140[399,159]D=21
#374[314,244]D=20
#349[301,235]D=20
#420[444,259]D=20
#159[451,172]D=18
#278[326,217]D=18
#424[351,260]D=18
#433[220,262]D=17
#429[212,258]D=17
#456[208,272]D=17
#169[401,177]D=17
#302[337,220]D=17
#223[408,201]D=17
#568[111,329]D=17
#266[158,211]D=17
#592[143,347]D=16
#530[319,310]D=16
#189[219,185]D=16
#534[116,312]D=16
#277[307,217]D=16
#31[442,111]D=16
#119[400,153]D=16
#208[410,192]D=16
#268[225,211]D=15
#403[363,253]D=15
```

Fig. 8. Example of an R-map plot, generated by GELLAB program DWRMAP, of T_0 P388D1 gel used for landmarking

Notice that the spots with labels are the largest (i.e., darkest) spots in the image. The numbers in the table on the right are the spot (CC number and *x*, *y*, and *D'*) values, in order of integrated spot density D'. The CC no. is the connected number of the component or spot relative to a particular gel segmentation. "Landmarking" two gels from these plots is done by manually tabulating a list of CC numbers for corresponding landmark spots. These lists can then be used to update the landmark data base by using the GELLAB program LMSEDIT

image from the original image. It is this last image that we use for estimating background—the zonal notch filter. A N × N window is moved through the image, stopping at each pixel where an average of non zero (i.e., background) pixel data is taken. This average is then used as an estimate of mean background. Taking the mode of the density histogram in each region would result in a slightly better estimate than does the mean in those cases where excessive "leakage" from a very dark spot occurs, as is sometimes found with spots such as actin in heavily exposed or loaded gels. Figures 7*d* and 7*e* show the zonal notch filter (contrast enhanced so that it could be photographed) for N = 16 and N = 32, respectively. Figure 7*f* shows the result of subtracting the 32 × 32 zonal notch filter background image from the original image (Figure 7*a*) resulting in minimized background variation.

Discussion

With such extensions to GELLAB as eR-spot sets and the C-gel′, it is now possible to investigate experimental gels more reliably than before and to contrast these experimental gels with a more stable estimate of the canonical gel map than the R-gel. Because the C-gel′ can be iteratively computed as new replicate control gels are produced, successively better estimates of the C-gel can be obtained, if the biochemistry involved and gel-production technology are stable and reproducible. GELLAB can currently accommodate up to 128 gels. This large capacity should not prevent one from considering the possibilities for decreasing the number of replications, both of controls and experimental gels required for statistical validation. In addition to the prospect of improved biochemical technique, leading to increased precision, another interesting facet is apparent. The C-gel′ construction allows, with appropriate (still to be determined in detail) statistical treatment, the iterative improvement of the parameters of the C-gel′—our approach to the model or canonical gel.

By thinking of selected spots in terms of sets and set operations, the biologist more easily can handle time- or dose-dependent variables in experiments involving sequences of gels. In such cases, each step in the sequence is defined as a different class, and the problem is recast as a problem in multiple-class analysis.

There still are problems in the reliable detection and accurate measurement of very light, very fuzzy, or noisy spots. These difficulties are reflected in false-positive or false-negative results. Although it is possible with this system to measure most spots that are visible to the human eye, in practice the uncertainty involved in evaluating such marginal spots precludes their consideration in an automated quantitative system. That is not to say that their qualitative consideration should be ignored or that improvements (through the use of replicate gels) cannot be obtained.

In addition, there is occasional mis-pairing. However, recent improvements in pairing algorithms (*19*) as well as those in progress in this laboratory should reduce this type of error.

Such is the generality of the various stages of analysis in GELLAB that, with little effort, data prepared by non-GELLAB programs could be used in succeeding stages of analysis with GELLAB. For example, alternatively derived procedures (e.g., manually measured or other segmentation and pairing algorithms) could be used in preparing paired-spot lists. These in turn can be read by CGELP to construct a data base. At this point, the analysis would continue as with GELLAB-prepared data.

GELLAB currently quantitates spots in terms of their total integrated density, which is expressed in optical density units relative to a given neutral-density step-wedge standard that is scanned along with the gels (it is visible at the bottom of some of the figures). However, with relatively minor changes in protocol (incorporation of radioactivity standards into the autoradiograph) and in some of the programs, results could be obtained in counts per minute. This is one of the changes we plan for 1982.

Current Status of the GELLAB System

GELLAB runs on the IPS DECsystem-2020 (under the TOPS-10 monitor) where picture input/output is provided by special hardware added to the system. However, in order to generalize and export GELLAB to other laboratories *without* special hardware, we have written several magnetic tape (magtape) and file-conversion programs, and these are being used to facilitate image acquisition and image transfer on other DECsystem computers. In particular: a magtape package exists to read Optronics scanner images produced by a PDP11 RT11 magtape system and convert them to GELLAB picture file format; a general-purpose image-conversion program converts various picture-file formats to or from the GELLAB picture-file format.

Because GELLAB is written in the SAIL programming language (*24*), it runs only on DECsystem-10 or DECsystem-20 computers (Digital Equipment Corp., Maynard, MA 01752). However, these medium-to-large main-frame time-shared computers currently are available at many places in this country, including some where time may be rented.

The hardware-independent portion of GELLAB has been supplied to the DCRT NIH computer center TOPS-10 system. In addition, the major portion of GELLAB has been supplied to the University of Chicago, running there on a DECsystem-2060 under the TOPS-20 operating system. Additional work is in progress to further image-exchange and graphics for the TOPS-20 version.

It is possible to use graphics plots for R-maps, mosaics, and landmarking rather than grey-scale images. One can thus use GELLAB without expensive raster grey-scale display hardware, although such grey-scale displays are the preferred mode of operation. Figure 8 illustrates an R-map of the gel-segmentation file produced by the gel-spot segmenter. Spots are represented as circles, the size of which is proportional to the spot's integrated density. By finding corresponding spots between R-maps for several gels, landmarking may be performed manually instead of by using the interactive grey-scale display hardware (*22*).

The current version of GELLAB is experimental and will soon be released to selected TOPS-10 DECsystem sites. Interested parties having access to a DECsystem-10 or -20 computer should contract the senior author for information regarding obtaining a free magtape copy of the runtime programs.

The constant help afforded by Morton Schultz, Bruce Shapiro, and Earl Smith, our colleagues in the Image Processing Section, has been invaluable. Marta Wade, also of the IPS, ran the tissue cultures on the P388D1 cell line. Our collaborators Snorri Thorgeirsson and Peter Wirth of NCI, and Carl Merril and David Goldman of NIMH have provided stimulating ideas and critical evaluation of the methodology as it has developed as well as running the 2D gels for the P388D1 experiments.

References

1. O'Farrell, P. H., High resolution two-dimensional electrophoresis of proteins. *J. Biol. Chem.* **250,** 4007–4021 (1975).

2. Anderson, N. G., and Anderson, N. L., Molecular anatomy. In *Behring Inst. Symposium 1977,* Mitt. 63, 169 (1979).

3. Lemkin, P., and Lipkin, L., GELLAB: A computer system for 2D gel electrophoresis analysis. I. Segmentation and system preliminaries. *Comp. Biomed. Res.* **14,** 272–297 (1981).

4. Lemkin, P., and Lipkin, L., GELLAB: A computer system for 2D gel electrophoresis analysis. II. Spot pairing. *Ibid.,* pp 355–380 (1981).

5. Lemkin, P., and Lipkin, L., GELLAB: A computer system for 2D gel electrophoresis analysis. III. Multiple gel analysis. *Ibid.,* pp 407–446 (1981).

6. Lipkin, L. E., and Lemkin, P. F., Data base techniques for two-dimensional polyacrylamide gel electrophoresis. *Clin. Chem.* **26,** 1403–1412 (1980).

7. Lester, E. P., Lemkin, P. F., and Lipkin, L. E., New dimensions in protein analysis. *Anal. Chem.* **53,** 390A–404A (1981).

8. Lemkin, P. F., and Lipkin, L. E., GELLAB: Multiple 2D electrophoretic gel analysis, In *Electrophoresis '81,* Allen and Arnaud, Eds., W. De Gruyter, New York, NY, in press.

9. Lemkin, P. F., and Lipkin, L. E., Database techniques for 2D electrophoretic gel analysis. In *Computing in Biological Science,* M.

Geisow and A. Barrett, Eds., Elsevier–North Holland, Amsterdam, in press.

10. Lemkin, P., *GELLAB User Manual*, NCI, Image Processing Section, NIH, Bethesda, MD, 1982.

11. Korfhage, R. F., *Logic and Algorithms*, J. Wiley & Sons, New York, NY, 1966.

12. Schwartz, A. A., and Soha, J. M., Variable threshold zonal filtering. *Appl. Opt.* **16,** 1779–1781 (1977).

13. Lipkin, L., Lemkin, P., Shapiro, B., and Sklansky, J., Preprocessing of electron micrographs of nucleic acid molecules for automatic analysis by computer. *Comp. Biomed. Res.* **12,** 279–289 (1979).

14. Lutin, W. A., Kyle, C. F., and Freeman, J. A., Quantitation of brain proteins by computer-analyzed two-dimensional electrophoresis. In *Electrophoresis '78*, N. Catsimpoolas, Ed., Elsevier–North Holland, Amsterdam, 1978, pp 93–106.

15. Garrels, J. I., Two-dimensional gel electrophoresis and computer analysis of proteins synthesized by clonal cell lines. *J. Biol. Chem.* **254,** 7961–7977 (1979).

16. Bossinger, J., Miller, M. J., Kiem-Phing, V., et al., Quantitative analysis of two-dimensional electrophoretograms. *J. Biol. Chem.* **254,** 7986–7998 (1979).

17. Vo, K-P, Miller, M. J., Geiduschek, E. P., et al., Computer analysis of two-dimensional gels. *Anal. Biochem.* **112,** 258–271 (1981).

18. Taylor, J., Anderson, N. L., Coulter, B. P., et al., Estimation of two-dimensional electrophoretic spot intensities and positions by modelling. In *Proceedings of Electrophoresis '79*, B. J. Radola, Ed., Walter de Gruyter, New York, NY, 1980, pp 329–339.

19. Taylor, J., Anderson, N. L., and Anderson, N. G., A computerized system for matching and stretching 2D gel patterns represented by parameter lists. In *Proceedings of Electrophoresis '81*, R. C. Allen and P. Arnaud, Eds., W. De Gruyter, New York, NY, In press.

20. Goldman, D., and Merril, C., Personal communication.

21. Nie, H. H., Hull, C. H., Jenkins, J. G., et al., *SPSS, a Statistical Package for the Social Sciences*, McGraw Hill, New York, NY, 1975.

22. Lemkin, P., Merril, C., Lipkin, L., et al., Software aids for the analysis of 2D gel electrophoresis images. *Comp. Biomed. Res.* **12,** 517–544 (1979).

23. Lipkin, L., Cellular effects of asbestos and other fibers: Correlations with in vivo induction of pleural sarcoma. *Environ. Health. Perspect.* **34,** 91–102 (1980).

24. Reiser, J. F., SAIL, Stanford University Artificial Intelligence Laboratory memo AIM-289, August 1976. [Also available from the U.S. Dept. Commerce., Nat. Tech. Inform. Serv. (No. AD-A045-102), Springfield, VA, 1976.]